On the Thermodynamics of Subduction

DAVID MARSHALL* AND JOHN MARSHALL

Department of Earth, Atmospheric, and Planetary Sciences, Massachusetts Institute of Technology, Cambridge, Massachusetts

(Manuscript received 16 December 1992, in final form 17 May 1994)

ABSTRACT

The thermodynamic processes attendant on the transfer of fluid between a surface mixed layer and a stratified thermocline beneath are discussed. For a parcel of fluid in the mixed layer to pass into the stratified thermocline—to subduct—it must be stratified by buoyancy input; this buoyancy can be supplied by local air–sea exchange and/or by lateral advective processes.

A series of experiments is described in which a mixed layer, coupled to an ideal-fluid thermocline, undergoes differing seasonal cycles: in one limit the mixed layer is held fixed in a steady, winter configuration; in the other the mixed layer is, more realistically, shallow over most of the year and deepens briefly in late winter. It is shown that the annual subduction rate S_{ann} depends, to first order, only on late winter mixed layer properties. However the annual-mean air–sea buoyancy exchange *is sensitive* to the details of the seasonal cycle and becomes vanishingly small as the effective subduction period shortens. In this limit the buoyancy is provided through advective processes in the Ekman layer.

The authors conclude that in ocean models that do not explicitly represent a seasonal cycle it is necessary to parameterize the process through a prescription of the winter mixed layer density and depth. The buoyancy forcing diagnosed from such models must be interpreted as the combined contribution of the annual air–sea exchange and lateral advective processes in the summer Ekman layer.

1. Introduction

The mixed layer, the interface between the stratified interior of the ocean and the atmosphere, rectifies the highly variable wind and buoyancy fluxes acting at the ocean's surface. The process by which fluid passes (subducts) from the mixed layer into the main thermocline of the subtropical gyre is intimately connected with both mechanical and thermodynamical forcing. The thermodynamics associated with subduction is the focus of attention here. For fluid in a cold, deep mixed layer to be absorbed into the stratified waters beneath, as illustrated schematically in Fig. 1, it must be restratified by warming. Fluid parcels in a weakly stratified mixed layer have small values of potential vorticity, which must be reset by a stratification process to allow the parcel to enter into the thermocline where the ambient potential vorticity is much higher. This restratification is thought to occur very rapidly, in a short period in the spring, when the mixed layer is warmed and shallowed. This heat can be supplied, as illustrated in Fig. 2, either by a flux through the sea surface or by a convergence of lateral heat fluxes in the Ekman layer[1] (see section 2). The relative importance of these two processes and the role of the seasonal cycle of the mixed layer in controlling them is addressed here.

Marshall et al. (1993, hereafter MNW) have diagnosed the subduction rate and period from North Atlantic climatology and discuss the attendant thermodynamic processes. The broad picture, as seen in Fig. 3, shows subduction rates of ~ 100 m yr^{-1} over the subtropical gyre, yet the annual mean net heat flux through the sea surface is close to zero. Over the subtropical gyre, the heat required to warm and shallow the mixed layer appears to be provided by advective heat transports associated with ageostrophic processes. Unambiguous interpretation of the data is made difficult, however, by the rather large uncertainties in the observed air–sea fluxes. Here we take an alternative

* Current affiliation: Department of Meteorology, University of Reading, United Kingdom.

Corresponding author address: David Marshall, Department of Meteorology, University of Reading, 2 Earley Gate, Whiteknights, P.O. Box 239, Reading, United Kingdom RG6 2AU.

[1] For convenience we occasionally refer to heat fluxes and warming/cooling. However, all our statements and equations have a straightforward and more general interpretation in terms of buoyancy fluxes, where

$$\mathcal{B} = -\frac{g\alpha_E}{\rho_0 C_w}\mathscr{H}$$

is the buoyancy flux equivalent to a heat flux $\mathscr{H}$. Here g is the gravitational acceleration, α_E is the expansion coefficient, C_w is the specific heat capacity, and ρ_0 the mean density of seawater.

© 1995 American Meteorological Society

Downloaded from http://journals.ametsoc.org/doi/pdf/10.1175/1520-0485(1995)025<0138:OTTOS>2.0.CO;2 by guest on 06 August 2020

approach, using an idealized time-dependent mixed-layer model coupled to a continuously stratified ideal-fluid thermocline, to study the thermodynamic aspects of subduction.

In section 2 the physical concepts with which we will be working are introduced. A continuously stratified thermocline model is formulated in section 3. The model incorporates a time-dependent mixed layer, driven by mechanical and diabatic forcing at the sea surface, and overlying a continuously stratified thermocline. In section 4, we present a series of solutions from the model designed specifically to elucidate the connections between subduction and the annual buoyancy forcing of the mixed layer. We find that the downward pumping of warm fluid from the summer Ekman layer into the seasonal thermocline provides the dominant buoyancy source for subduction. Implications of our results for models with no seasonal cycle are discussed in section 5.

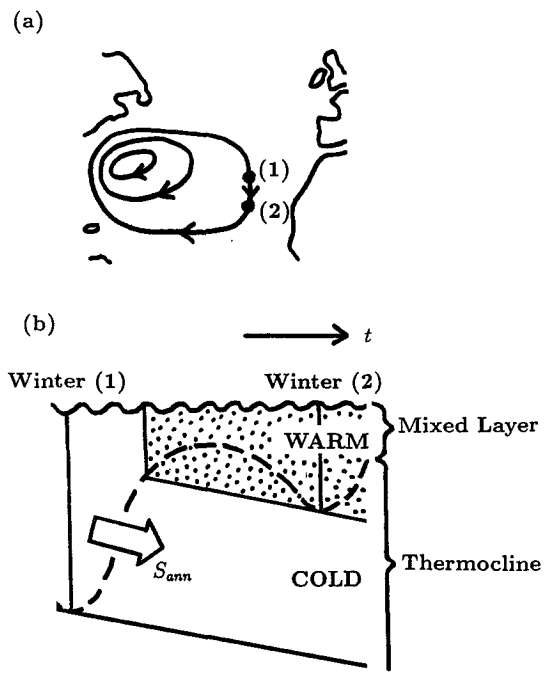

FIG. 1. A schematic diagram showing how cold mixed layer fluid must be restratified by warming in order to be absorbed into the main thermocline. (a) We consider a column of fluid as it migrates equatorward in the subtropical gyre between winter (1) and winter (2). (b) The time evolution of the fluid column over the year: Ekman pumping drives fluid downward and, through the Sverdrup relation, southward. In summer the mixed layer is warmed and shallowed, while in winter it is cooled and deepened. However, the mixed layer experiences a residual warming and shallowing as it migrates to more southerly latitudes, thereby enabling denser fluid to subduct into the main thermocline. The mixed layer base is denoted by the dashed line, and isopycnals are denoted by solid lines. The annual rate at which vertically homogeneous mixed layer fluid is converted to stratified thermocline fluid is given by S_{ann}.

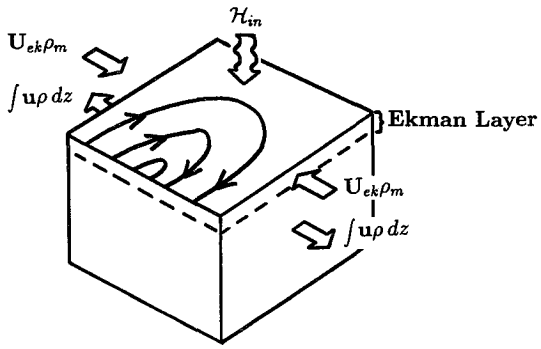

FIG. 2. The heat necessary to restratify the fluid column can be provided by either (i) a flux through the sea surface, $\mathscr{H}_{in}$ or (ii) a net accumulation of buoyancy within the gyre due to an influx of buoyant fluid in the surface Ekman layer.

2. Physical concepts

Consider a Lagrangian column of fluid circulating with the geostrophic flow in the subtropical gyre, exposed at its surface to a seasonal buoyancy and wind forcing as shown schematically in Fig. 1: the column extends from the sea surface to the base of the seasonal thermocline. Ekman pumping over the subtropical gyre drives fluid downward and, in accord with the Sverdrup relation, southward. Typical climatological vertical velocities are 60 m yr^{-1}, and this induces a southward velocity sufficient to move a fluid column ~500 km in one year. So particles of fluid glide down on gently inclined surfaces. However, as the particle migrates to more southerly latitudes, the mixed layer warms and shallows allowing colder fluid to pass irreversibly into the main thermocline (Woods 1985) (See Fig. 1b).

The heat stored within the fluid column can be modified by two distinct mechanisms (Fig. 4a): a heat flux across the sea surface $\mathscr{H}_{in}$ at $z = 0$ and/or a convergence of advective buoyancy fluxes within the fluid column[2]

$$\frac{D}{Dt}\int_{z_s}^{0}\left(-\frac{C_w}{\alpha_E}\rho\right)dz = \mathscr{H}_{in} + \frac{C_w}{\alpha_E}\{\nabla\cdot(\mathbf{U}_{Ek}\rho_m) - w_{Ek}\rho_s\}. \quad (1)$$

Here ρ_m is the mixed layer density, ρ_s is the density of fluid at the base of the seasonal thermocline ($z = z_s$), $\mathbf{U}_{Ek}$ is the ageostrophic Ekman transport, w_{Ek} is the vertical Ekman pumping velocity, α_E is the expansion coefficient, and C_w is the specific heat capacity of seawater.

[2] We assume that our column is advected around the gyre with a velocity set by the geostrophic current averaged over the depth of the column. Furthermore, the contribution to the thermodynamic budget associated with deviations from this barotropic current, i.e., baroclinic advection is negligible. This is discussed in more detail, and estimates are given of the size of neglected terms in the appendix of MNW. They show that an error is committed equivalent to only ~4 W m^{-2}.

Downloaded from http://journals.ametsoc.org/doi/pdf/10.1175/1520-0485(1995)025<0138:OTTOS>2.0.CO;2 by guest on 06 August 2020

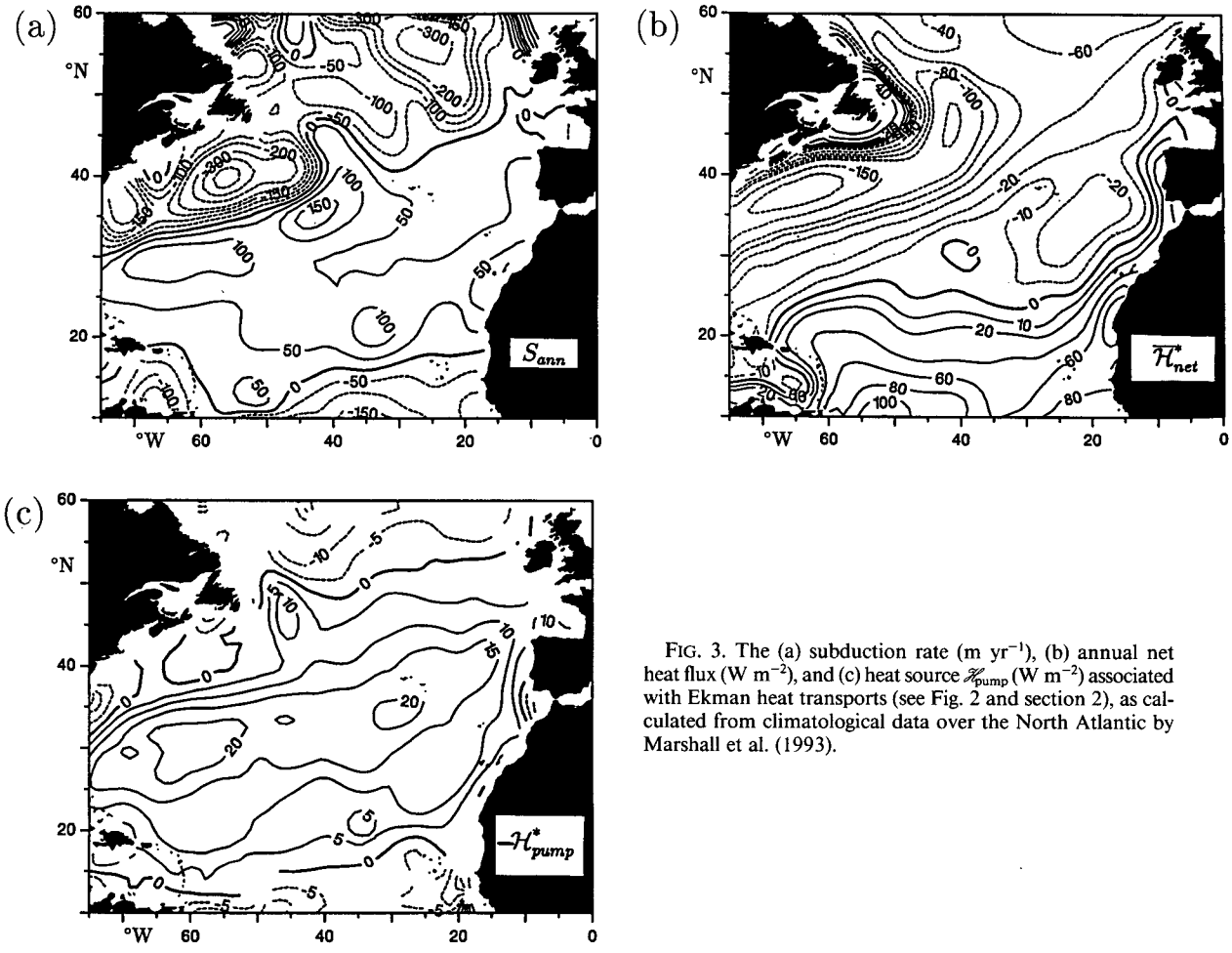

FIG. 3. The (a) subduction rate (m yr^{-1}), (b) annual net heat flux (W m^{-2}), and (c) heat source $\mathcal{H}_{pump}$ (W m^{-2}) associated with Ekman heat transports (see Fig. 2 and section 2), as calculated from climatological data over the North Atlantic by Marshall et al. (1993).

It is convenient to focus on that part of the fluid column beneath the surface Ekman layer (Fig. 4b), in which case the budget becomes

$$\frac{D}{Dt}\int_{z_s}^{z_{Ek}}\left(-\frac{C_w}{\alpha_E}\rho\right)dz = \mathcal{H}_{net} - \frac{C_w}{\alpha_E} w_{Ek}(\rho_s - \rho_m), \quad (2)$$

where $\mathcal{H}_{net}$ is the heat flux through the base of the Ekman layer ($z = z_{Ek}$) and $(C_w/\alpha_E)\, w_{Ek}(\rho_m - \rho_s)$ is the heat gain due to the convergence of advective fluxes. Since the heat stored in the thin Ekman layer is a small fraction of the total heat stored in the column, we equate the rhs of Eqs. (1) and (2) and, noting $\nabla \cdot \mathbf{U}_{Ek} = w_{Ek}$, deduce that

$$\mathcal{H}_{net} = \mathcal{H}_{in} + \frac{C_w}{\alpha_E}\mathbf{U}_{Ek}\cdot\nabla\rho_m; \quad (3)$$

$\mathcal{H}_{net}$ is the heat flux available for subduction: the heat flux through the sea surface plus the advection of heat by the Ekman transport. In a steady model there is no seasonal thermocline, that is, $\rho_s = \rho_m$, and therefore the second term in (2) vanishes. However, in the presence of a realistic seasonal cycle, we will show that this term makes the largest contribution to the buoyancy of the fluid column, dominating the annual mean $\mathcal{H}_{net}$.

We now discuss in more detail the contribution of the two buoyancy sources in Eq. (2) to the subduction/restratification mechanism.

a. Instantaneous subduction

The subduction rate, defined kinematically as

$$S = -\left(\frac{D_b h}{Dt} + w_b\right) \quad (4)$$

(Cushman-Roisin 1987), describes the instantaneous rate at which mixed layer fluid is converted into stratified thermocline fluid. Here D_b/Dt and w_b are the Lagrangian time derivative and the vertical velocity at the base of the mixed layer at a depth $z = h$.

For a parcel of fluid in the mixed layer to "subduct" into the seasonal thermocline, it must be restratified through warming. Entrainment fluxes are zero during periods of subduction since the mixed layer is warming

Downloaded from http://journals.ametsoc.org/doi/pdf/10.1175/1520-0485(1995)025<0138:OTTOS>2.0.CO;2 by guest on 06 August 2020

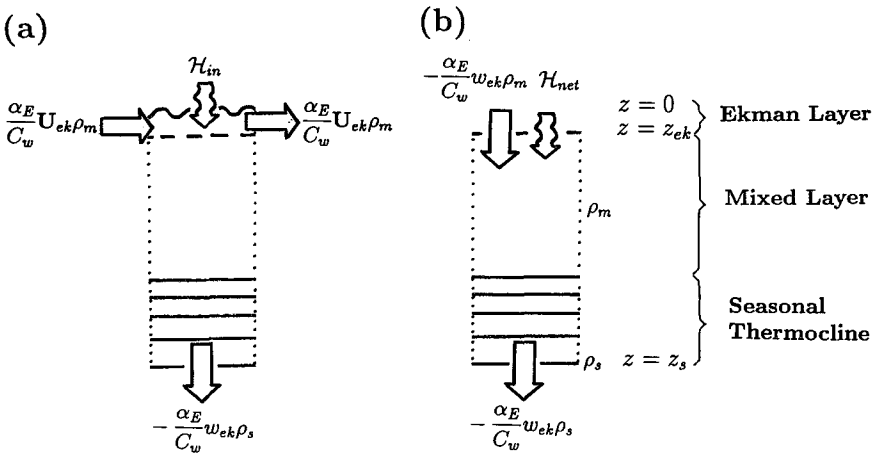

FIG. 4. (a) The heat budget of a Lagrangian column of fluid that extends from the sea surface to the base of the seasonal thermocline. The total heat stored within the fluid column can be modified by a flux of heat $\mathcal{H}_{in}$ through the sea surface and/or a net advection of heat into the fluid column. Here $(\alpha_E/C_w)\nabla\cdot(U_{Ek}\rho_m)$ is the convergence of heat into the column within the surface Ekman layer, and $-(\alpha_E/C_w)w_{Ek}\rho_s$ is the vertical advective flux at the base of the column $z = z_s$, where $\rho = \rho_s$. (b) The heat budget of the Lagrangian column beneath the surface Ekman layer. The heat flux "available for subduction" is $\mathcal{H}_{net}$, to which must be added a vertical advection of heat $(\alpha_E/C_w)w_{Ek}\rho_m$.

and shallowing. The rate at which mixed layer fluid is converted to stratified thermocline fluid is therefore proportional to the net heat flux $\mathcal{H}_{net}$ through the relation

$$S = \frac{\alpha_E f \mathcal{H}_{net}}{C_w h Q_b}, \tag{5}$$

where h is the depth of the mixed layer and Q_b is the potential vorticity at its base. (See Nurser and Marshall 1991 or Marshall and Nurser 1992 for a derivation.) Equation (5) emphasizes and makes explicit that there are important thermodynamic processes attendant on subduction. This connection with thermodynamics is hidden in the kinematic definition, Eq. (4): the mixed layer base is a material surface (i.e., $w_b = -D_b h/Dt$) in the absence of diabatic processes.

However, the quantity of importance for the main thermocline is not the instantaneous rate at which mixed layer fluid is converted into stratified thermocline fluid but rather the *annual* subduction rate S_{ann} at which fluid passes into the main thermocline.

b. Annual subduction

Restratification occurs during a relatively short period in spring, in which the mixed layer shallows and warms. Following Stommel (1979) and Cushman-Roisin (1987), we define an "effective subduction period," t_{eff}, during which fluid that is subducted will escape irreversibly into the main thermocline (Fig. 5). MNW show in their diagnostic study that t_{eff} is typically as short as one month over the subtropical gyre. Outside of this period, fluid is subducted only to be reentrained again as the mixed layer deepens with the onset of winter. Thus, S_{ann} is equal to the integral of S over the subduction period

$$S_{ann} = \int_0^{t_{eff}} S dt = \int_0^{t_{eff}} \frac{\alpha_E f \mathcal{H}_{net}}{C_w h Q_b} dt. \tag{6}$$

During this period, the mixed layer is warmed from a density $\rho_m(t = 0)$ to $\rho_m(t = t_{eff}) \equiv \rho_m(t = 1)$ (Fig. 5), where time is normalized with respect to a year. The heat flux required, which we call $\mathcal{H}_{sub}$, is

$$\mathcal{H}_{sub} = \int_0^{t_{eff}} \mathcal{H}_{net} dt. \tag{7}$$

But how is $\mathcal{H}_{sub}$ related to the annual cycle of buoyancy fluxes into the fluid column?

If there were no seasonal cycle, then $\mathcal{H}_{sub}$ would simply be the annual-mean net heat flux. With a realistic seasonal cycle, however, the vertical advective terms in (2) can make an important contribution to $\mathcal{H}_{sub}$. As indicated schematically in Fig. 5, the column can be warmed by the pumping down of fluid from the summer Ekman layer into the seasonal thermocline. This fluid is anomalously warm relative to the fluid that subducts into the main thermocline. The resultant heat gain of the fluid column causes the mixed layer to warm and shallow, even in the absence of annual mean net heating. As shown by Federiuk and Price (1985, unpublished manuscript) using a one-dimensional mixed layer model, and as suggested by the data analysis of MNW, this process can supply the major part of the buoyancy required to support the annual subduction rate.

Downloaded from http://journals.ametsoc.org/doi/pdf/10.1175/1520-0485(1995)025<0138:OTTOS>2.0.CO;2 by guest on 06 August 2020

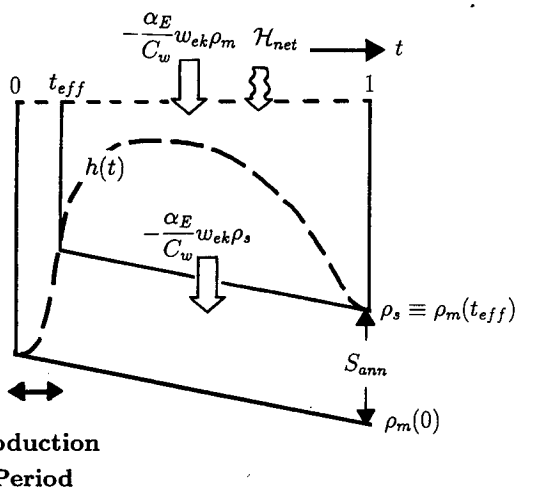

FIG. 5. A schematic diagram illustrating the annual subduction mechanism and its attendant thermodynamics. The figure shows the time evolution of a fluid column between two winters, $t = 0$ and $t = 1$. The mixed-layer base $h(t)$ is the dashed line, and solid lines are isopycnals. Subduction occurs during a short "effective subduction period," $t = 0 \rightarrow t_{\text{eff}}$, in spring when the mixed layer is warmed and shallowed. Fluid that is subducted outside of this period is subsequently reentrained when the mixed layer deepens later in the year. During the effective subduction period, the mixed layer is warmed from a density $\rho_m(0)$ to a density $\rho_s \equiv \rho_m(t_{\text{eff}})$. The heat that makes this subduction possible $\mathcal{H}_{\text{sub}}$ is provided by both the annual net heat flux and also the vertical pumping term, $-(\alpha_E/C_w)w_{\text{Ek}}\{\rho_s - \rho_m(t)\}$. This latter term makes a large contribution during summer months when *warm* water is pumped from the Ekman layer into the *cooler* seasonal thermocline.

More quantitatively, the annual buoyancy supplied to the fluid column extending from the base of the Ekman layer to the base of the seasonal thermocline is given by (as is evident from Fig. 5)

$$\mathcal{H}_{\text{sub}} = \overline{\mathcal{H}_{\text{net}}} - \mathcal{H}_{\text{pump}}, \tag{8a}$$

where

$$\mathcal{H}_{\text{pump}} = \frac{C_w}{\alpha_E} \int_{t_{\text{eff}}}^{1} w_{\text{Ek}}\{\rho_s - \rho_m(t)\}\, dt \tag{8b}$$

is the quantity introduced and calculated from climatological data by MNW (see Fig. 3) and the overbar denotes the annual mean.

We now wish to study the relative importance of these two buoyancy sources, $\overline{\mathcal{H}_{\text{net}}}$ and $\mathcal{H}_{\text{pump}}$, to the subduction mechanism and how this depends on the details of the seasonal cycle. This involves the development of a thermocline model that can explicitly represent the interaction of a time-dependent, thermodynamically forced mixed layer with a continuously stratified thermocline. Readers who are not interested in the details of the model can move directly to section 4.

3. The model

Our model, an extension of that introduced by Marshall and Nurser (1991), incorporates a surface mixed layer of variable density ρ_m and depth $z = -h$, overlying a continuously stratified ideal-fluid thermocline; see Fig. 6. It is driven by wind and buoyancy forcing at the sea surface. Within the thermocline, motion is restricted to fluid contained within a bowl $z = -D$, which does not interact with the ocean floor; beneath the bowl fluid is at rest and density takes up a reference value $\rho = \rho_0(z)$.

We first outline the physics of our model incorporating full time dependence and fairly general mixed layer physics. We subsequently introduce two simplifications that considerably reduce the computational effort required to find solutions but retain the essential physics of the subduction mechanism and attendant thermodynamic processes.

a. Dynamical balances

1) THE MIXED LAYER

We suppose that the mixed layer is a vertically homogeneous layer of density ρ_m and thickness h, exposed at its surface to diabatic and mechanical forcing. Ageostrophic motion due to the surface wind forcing is confined to a thin Ekman layer, while diabatic forcing acts throughout the mixed layer. The geostrophic mixed layer velocity $\mathbf{u}_m$ can be expressed as the sum of the surface velocity and the thermal wind

$$\mathbf{u}_m = \frac{1}{\rho_0 f}\,\mathbf{k} \times \nabla p_s - \frac{gz}{\rho_0 f}\,\mathbf{k} \times \nabla \rho_m,$$

where p_s is the surface pressure, f is the Coriolis parameter, and g is the gravitational acceleration. Note

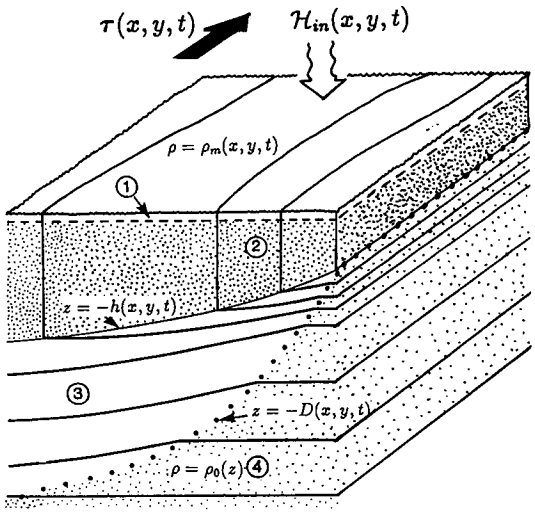

FIG. 6. A schematic diagram of the model. A wind stress τ and a heat flux $\mathcal{H}_{\text{in}}$, are prescribed at the sea surface. Mechanical forcing is confined to a thin surface Ekman layer (1), and thermal forcing to the vertically homogeneous mixed layer (2) of depth h and density ρ_m. The main thermocline (3) in which there is motion is separated from a motionless abyss (4) by a bowl of depth $z = -D$.

Downloaded from http://journals.ametsoc.org/doi/pdf/10.1175/1520-0485(1995)025<0138:OTTOS>2.0.CO;2 by guest on 06 August 2020

that the thermal wind component cannot advect the mixed layer density field, and so the thermodynamic balance of the mixed layer can be written

$$h\frac{\partial \rho_m}{\partial t} + \frac{h}{\rho_0 f}\mathbf{k}\times\nabla p_s\cdot\nabla\rho_m + \mathbf{U}_{\mathrm{Ek}}\cdot\nabla\rho_m = -\frac{\alpha_E}{C_w}\mathscr{H}_{\mathrm{in}} + S(\Delta\rho)_b, \quad (9)$$

where $\mathbf{U}_{\mathrm{Ek}} = (1/\rho_0 f)\mathbf{k}\times\boldsymbol{\tau}$ is the ageostrophic transport carried by the Ekman layer, $\boldsymbol{\tau}$ is the surface wind stress, $\mathscr{H}_{\mathrm{in}}$ is the heat flux through the ocean surface, S is the subduction rate as defined by Eq. (4), and $(\Delta\rho)_b$ is the discontinuity in density at the base of the mixed layer. The mixed layer density is thus modified by geostrophic advection, advection by the ageostrophic Ekman fluxes, a flux of buoyancy through the sea surface, and entrainment of fluid from the seasonal thermocline.

2) THE THERMOCLINE

The thermocline consists of two regions separated by a bowl $z = -D(x, y, t)$ across which density and pressure are continuous, as first exploited in the model of Rhines and Young (1982). Beneath the bowl, fluid is assumed at rest,[3] and pressure, density, and the depth of an isopycnal surface take up reference values:

$$p = p_0(z), \quad \rho = \rho_0(z), \quad z = z_0(\rho). \quad (10)$$

Above the bowl, the flow is in geostrophic and hydrostatic balance and conserves density. It follows that the potential vorticity is conserved following the motion

$$\frac{\partial Q}{\partial t} + \mathbf{u}\cdot\nabla Q = 0, \quad (11)$$

where

$$Q = -f\frac{\partial\rho}{\partial z} \quad (12)$$

is the potential vorticity appropriate to the planetary scale and

$$\mathbf{u} = \frac{1}{\rho_0 f}\mathbf{k}\times\nabla_\rho M. \quad (13)$$

Here $M(x, y, \rho) = p + \rho g z(\rho)$ is the Montgomery potential, and the gradient operator ∇_ρ is evaluated on an isopycnal surface.

3) SVERDRUP BALANCE

We suppose further that the meridional transport of the gyre is constrained by linear vorticity balance,

$$\beta\int_{-D}^{0} v\,dz = f w_{\mathrm{Ek}}, \quad (14)$$

where $w_{\mathrm{Ek}} = \mathbf{k}\cdot\nabla\times(\boldsymbol{\tau}/\rho_0 f)$ is the vertical Ekman pumping velocity at the base of the surface Ekman layer and w vanishes on the bowl. A complete specification of both the potential vorticity field of the thermocline, through prognostic integration of Eq. (11), and the mixed layer density field, through integration of Eq. (9), enables calculation of the baroclinic component of the horizontal fluid velocity throughout the gyre. Given the pattern of Ekman pumping, the meridional component of the depth-integrated transport is determined from Eq. (14). The one remaining degree of freedom is the zonal transport of the gyre, and this is fixed by invoking continuity and imposing an eastern boundary condition. We choose to set the bowl depth equal to the mixed layer depth,

$$D(x_e, y) = h(x_e, y), \quad (15)$$

implying a (what will turn out to be) small geostrophic mixed layer transport into the eastern boundary.

b. Model simplifications

The thermocline model outlined above possesses a complexity intermediate to that of steady thermocline theory of Rhines and Young (1982) and Luyten et al. (1983) and the primitive equation isopycnic model of Bleck et al. (1989), for example. Nevertheless, its solution involves prognostic integration for the full three-dimensional potential vorticity field of the main thermocline. However, because our primary goal here is to study the association between subduction and buoyancy forcing of the mixed layer, we now introduce two further assumptions, which allow us to tremendously simplify our model—in fact, reduce it to the solution of a *single* characteristic equation for ρ_m—and yet not prejudice its use for study of the problem at hand.

1) THE MIXED LAYER CYCLE

As shown in section 2b, the annual subduction rate is related to the annual input of buoyancy into the fluid column extending from the sea surface to the base of the seasonal thermocline. Penetrative mixing, driven by turbulent kinetic energy input from surface winds or vigorous convective overturning, helps to deepen and, through the entrainment of denser fluid from the seasonal thermocline waters, to cool the mixed layer.

[3] In principle, as the bowl moves up and down, Rossby waves will be radiated into the stagnant fluid beneath. However, the bowl depth is predominantly a function of the surface wind forcing, which does not vary here; indeed, we find that the seasonal variation in the depth of the bowl is less than 50 m over most of the gyre (estimates are given in Marshall and Nurser 1991). A more complete treatment of the generation of Rossby waves induced by a seasonally varying surface buoyancy forcing is given by Liu and Pedlosky (1994) using a two-layer model coupled with a surface mixed layer. They confirm that variability arising from time-dependent buoyancy forcing is predominantly confined to the mixed layer and ventilated thermocline.

Downloaded from http://journals.ametsoc.org/doi/pdf/10.1175/1520-0485(1995)025<0138:OTTOS>2.0.CO;2 by guest on 06 August 2020

However, the net buoyancy stored in the fluid column is *not* modified by penetrative mixing: buoyancy is merely redistributed *between* the mixed layer and seasonal thermocline.[4] We therefore choose to ignore penetrative mixing altogether and set $(\Delta\rho)_b = 0$ throughout the entire year.

2) THE POTENTIAL VORTICITY FIELD

The potential vorticity of subducted fluid is determined by the rate at which the mixed layer shallows relative to the rate at which the mixed layer warms:

$$Q_b = f\,\frac{\partial\rho_m/\partial t + \mathbf{u}_b\cdot\nabla\rho_m}{\partial h/\partial t + \mathbf{u}_b\cdot\nabla h + w_b} \qquad (16)$$

(Cushman–Roisin 1987; Williams 1991). In principle one should solve for Q_b using Eq. (16). However, in order to sidestep the technical challenge of incorporating Rossby waves into our solutions, and the associated intensive computation involved in prognostic integration of the three-dimensional potential vorticity field of the main thermocline, we will assume here that potential vorticity is uniform on each density surface within the thermocline. This idea, of course, has been employed many times before, notably by Rhines and Young (1982). The uniform potential vorticity assumption leads to a somewhat artificial coupling between the mixed layer density and depth in our solutions, but the assumption in no sense corrupts those aspects of the subduction mechanism and the associated thermodynamics that are the focus of attention here. The seasonal cycle in our model, and in the ocean, is driven by the cycle of buoyancy forcing; while the cycle will excite Rossby waves (e.g., Dewar 1989), they are a consequence of the cycle rather than its cause, and we therefore feel justified in excluding them.

c. *Method of solution*

The above simplifying assumptions enable us, as shown in Marshall and Nurser (1991), to reduce the entire problem, set out in sections 3a and 3b, to the solution of a single characteristic equation in the mixed layer density alone (details are given in the appendix):

$$\frac{\partial\rho_m}{\partial t} + \mathbf{u}_c\cdot\nabla\rho_m = \mathcal{F}, \qquad (17)$$

where

$$\mathbf{u}_c = \frac{1}{\rho_0 f}\,\mathbf{k}\times\nabla p_s + \frac{1}{h}\,\mathbf{U}_{\mathrm{Ek}},$$

is the characteristic velocity, and

$$\mathcal{F} = -\frac{\alpha_E \mathscr{H}_{\mathrm{in}}}{C_w h}.$$

Equation (17) can be stepped forward in time for a new field of ρ_m by integrating along characteristics; thus,

$$\rho_m(t + \Delta t, \mathbf{x} + \mathbf{u}_c\Delta t) = \rho_m(t, \mathbf{x}) + \mathcal{F}(t + \Delta t/2, \mathbf{x} + \mathbf{u}_c\Delta t/2)\Delta t. \qquad (18)$$

Solutions driven by prescribed patterns of wind and buoyancy forcing are presented in Marshall (1992). Here we restrict our attention to solutions in which a mixed layer cycle is imposed a priori: instead, we employ Eq. (18) to diagnose the surface heat flux.

4. Subduction experiments

Idealized subduction experiments are now presented for a subtropical gyre circulating in a basin of dimension 5000 km × 3000 km that is open to the west at $x = 0$; solid boundaries are assumed at $x = x_e$, $y = y_s$, y_n. The Ekman pumping velocity varies sinusoidally with latitude:

$$w_{\mathrm{Ek}} = w_0 \sin\left\{\pi\left(\frac{y_n - y}{y_n - y_s}\right)\right\},$$

where $w_0 = -2\times10^{-6}$ m s^{-1} corresponding to a maximum downward pumping of ~60 m yr^{-1}. A linear reference stratification is assumed,

$$\rho_0(z) = a - bz,$$

where $a = 1026.6$ kg m^{-3} and $b = 2\times10^{-3}$ kg m^{-4}. We homogenize potential vorticity to the same value on each density surface:

$$Q = -f(y_n)\,\frac{d\rho_0}{dz}.$$

The Coriolis parameter is assigned a value $f(y_n) = 0.9\times10^{-4}$ s^{-1} on the northern boundary of the gyre, appropriate to a latitude of ~40°N, and the planetary vorticity gradient is $\beta = 2.1\times10^{-11}$ m^{-1} s^{-1}. Other parameters have values: $\alpha_E = 2.0\times10^{-4}$ K^{-1}, $C_w = 3.9\times10^{3}$ J kg^{-1} K^{-1}.

a. *The mixed layer cycles*

We present three idealized experiments: the first (experiment 1) is the steady limit in which the mixed layer has late winter properties all the year around; the second (experiment 2) is an intermediate case in which the mixed layer spends an equal amount of time in deep winter and shallow summer configurations; in the third (experiment 3), the mixed layer is shallow for most of the year and deep for approximately one month. More quantitatively, our chosen mixed layer depth cycles, plotted in Fig. 7a, are

[4] A reviewer has noted that penetrative mixing will induce a small change in $\mathscr{H}_{\mathrm{pump}}$, as defined in Eq. (8b), since ρ_m is increased by the entrainment of denser thermocline fluid.

Downloaded from http://journals.ametsoc.org/doi/pdf/10.1175/1520-0485(1995)025<0138:OTTOS>2.0.CO;2 by guest on 06 August 2020

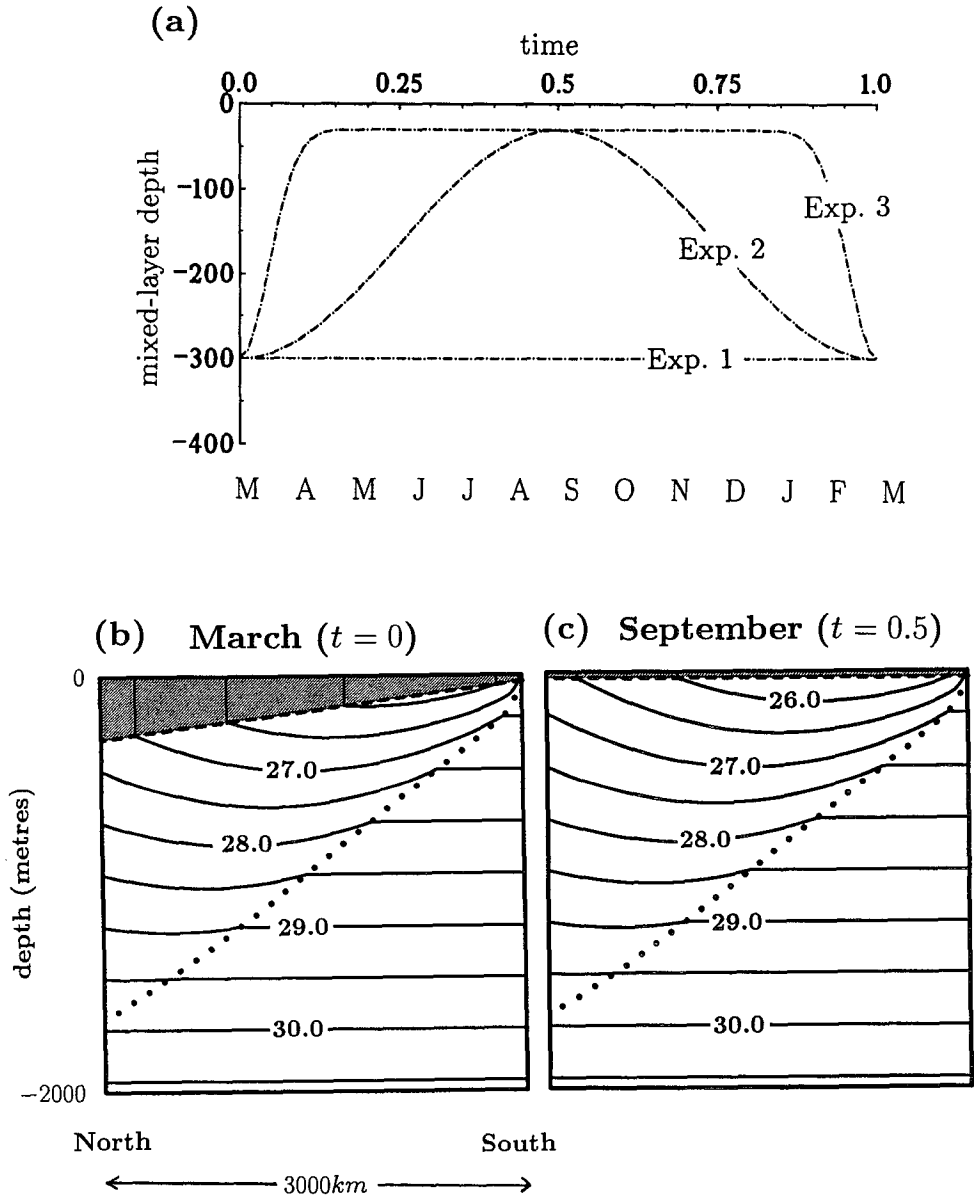

FIG. 7. The mixed layer cycles in the three experiments. (a) The variation of h with time on the northern boundary of the gyre in each experiment. Time $t = 0$ is defined as March when the mixed layer is deepest, and the months of the year are indicated by letters at the bottom of the diagram. (b) A hydrographic section through the gyre at its western boundary in March ($t = 0$). (c) The same section in September ($t = 0.5$). The mixed layer is shaded gray, and the bowl is indicated by the dotted line.

$$h(x, y, t) = h_{\min} + (h_{\max} - h_{\min})\left(\frac{y - y_s}{y_n - y_s}\right)\cos^{2n}\omega t,$$

where $n = 0$, 1, and 25, for experiments 1, 2, and 3, respectively. Here $h_{\min} = 30$ m is the uniform depth of the mixed layer in late summer, and $h_{\max} = 300$ m is the maximum depth achieved by the mixed layer on the northern boundary in winter. The variation in mixed-layer depth is linear with latitude; on the southern boundary there is no seasonal cycle. Hydrographic sections along the western boundary gyre are shown in Fig. 7b (winter, $t = 0$) and Fig. 7c (summer, $t = 0.5$); these extreme winter and summer mixed layers are the same in each experiment.

1) SUBDUCTION RATES

One might initially suppose that the annual mass flux of water subducted into the permanent thermocline, S_{ann}, could be evaluated by simply taking the time average of S across the instantaneous base of the

Downloaded from http://journals.ametsoc.org/doi/pdf/10.1175/1520-0485(1995)025<0138:OTTOS>2.0.CO;2 by guest on 06 August 2020

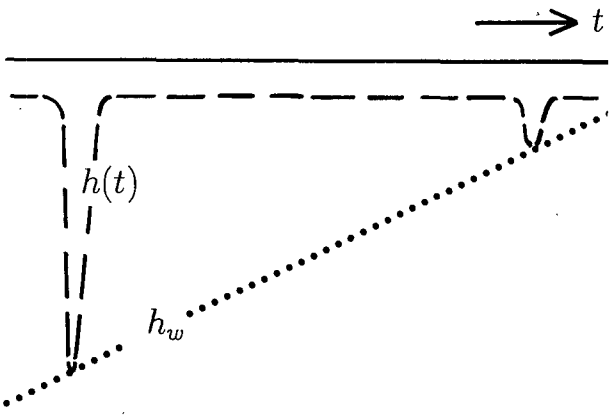

FIG. 8. A thought experiment that demonstrates the difference between the annual subduction rate S_{ann} and the annual-mean flux through the base of the instantaneous mixed layer $\bar{S}$. We assume that the mixed layer is uniformly shallow for all but one day each year, during which the surface water is mixed down to a large depth that varies horizontally. Assuming, for convenience, that the circulation is independent of depth, it is clear that lateral advection makes little contribution to $\bar{S} = -(\mathbf{u}\cdot\nabla\bar{h} + w)$, since $\nabla\bar{h} \approx 0$. Nevertheless, a substantial volume of water is swept laterally through the sloping interface defined by the deepest winter mixed layer, $z = -h_w$, thereby contributing significantly to the annual subduction rate, $S_{ann} = -(\mathbf{u}\cdot\nabla h_w + w)$.

mixed layer—the dashed line in Fig. 8. However, this is not the case. Consider the following thought experiment, outlined in Fig. 8, in which the mixed layer is uniformly shallow for all but one day each year when surface water is mixed to a large (but spatially nonuniform) depth. The *time-mean* subduction rate is

$$\bar{S} = -(\overline{\mathbf{u}_b\cdot\nabla h + w_b}),$$

where $\mathbf{u}_b$ and w_b are the horizontal and vertical velocity components at the base of the instantaneous mixed layer $z = -h(t)$. The time-mean gradient in the mixed layer depth is close to zero, and therefore $\bar{S}$ is dominated entirely by the vertical velocity $\overline{w_b}$. However, as is evident from Fig. 8, a substantial volume of water must escape into the permanent thermocline by lateral motion through the interface defined by the base of the deepest winter mixed layer. The *annual* subduction S_{ann} is therefore much larger than the time mean of S.

If we define the permanent thermocline as that portion of the stratified column that is shielded from surface forcing throughout the year, then the annual rate per unit surface area at which fluid subducts into the main thermocline is unambiguously defined as

$$S_{ann} = -(\overline{\mathbf{u}_w}\cdot\nabla h_w + \overline{w_w}). \qquad (19)$$

Here $\mathbf{u}_w$, w_w are the annual-mean velocity components on the Eulerian interface $z = -h_w(x, y)$ (the dotted line in Fig. 8) representing the base of the deepest winter mixed layer, the interface between the seasonal and permanent thermoclines. Note that there are no eddy contributions to (19) because h_w is an Eulerian interface. Equation (19) is the appropriate definition of the annual subduction rate because it explicitly quantifies the volume of fluid passing into the permanent thermocline.

Since the structure of the winter mixed layer is identical in each experiment, the annual subduction rate is virtually independent of the detailed seasonal cycle, see Fig. 9, and reaches the same maximum of ~70 m yr^{-1} in each case.

2) SUBDUCTION PERIODS

Subduction periods for the three experiments are shown in Fig. 10 and have been calculated by tracking

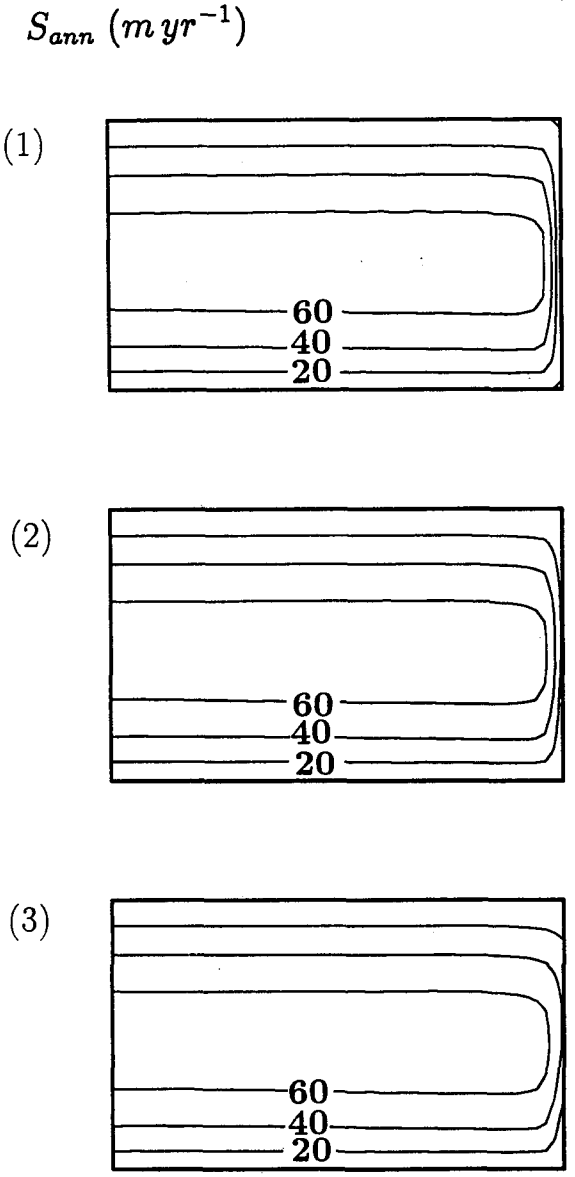

FIG. 9. The annual subduction rate S_{ann} (m yr^{-1}) in each of the experiments.

Downloaded from http://journals.ametsoc.org/doi/pdf/10.1175/1520-0485(1995)025<0138:OTTOS>2.0.CO;2 by guest on 06 August 2020

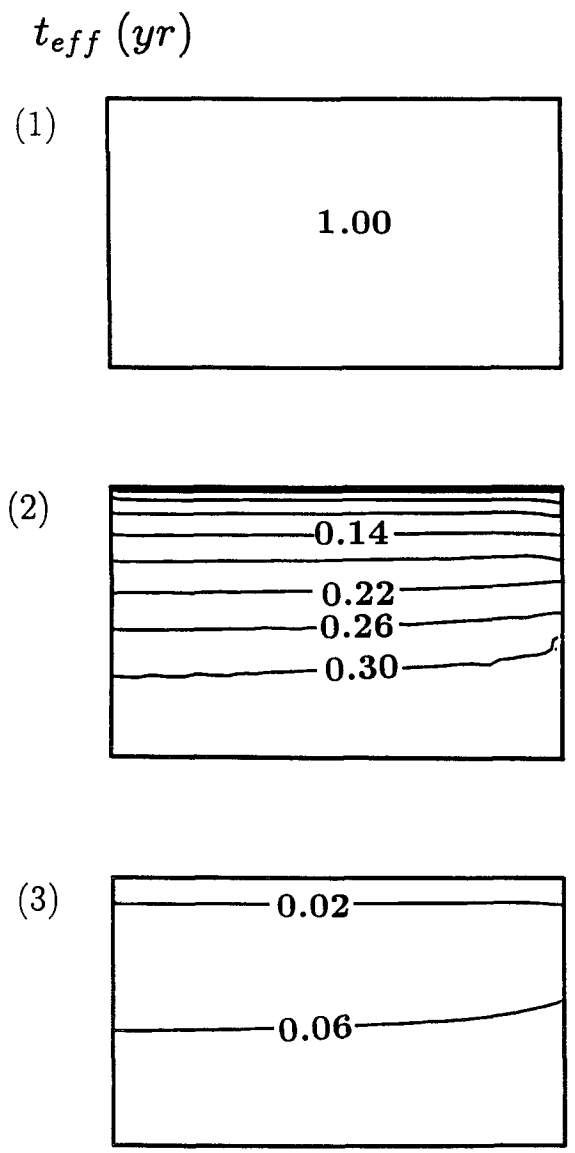

FIG. 10. Effective subduction periods in fractions of a year for each experiment: t_{eff} ranges from the whole year in experiment 1 in which the mixed layer is steady, to less than a month in experiment 3 where the mixed layer shallows rapidly in spring.

fluid parcels that are on the threshold of irreversible subduction. The first experiment corresponds to the steady limit, as exploited by previous authors, in which the mixed layer has late winter properties: subduction occurs over the entire year. In experiment 2, the mixed layer spends an equal amount of time in winter and summer configurations: the subduction period ranges from two to four months over most of the gyre. The third experiment is characterized by a short season of deep mixing: the effective subduction period is now less than a month due to the rapid surfacing of the mixed layer in spring. The subduction period is observed to be of the order of a month over much of the subtropical gyre (MNW).

It is important to note that while the flux of mass into the main thermocline is the same in each experiment, the properties of the subducted fluid will be rather different due to the different subduction periods (Stommel 1979; Williams et al. 1994). In experiment 1 they will correspond to the range of properties of the mixed layer over the entire year, while in experiment 3 they will correspond exclusively to mixed layer properties in March.

b. The annual buoyancy budget of the mixed layer

In section 2, we introduced the heat flux $\mathscr{H}_{\text{sub}}$ required to reset the potential vorticity of fluid that is irreversibly subducted from the vertically homogeneous mixed layer into the stratified thermocline. We plot $\mathscr{H}_{\text{sub}}$ in Fig. 11 from each of our idealized experiments: there is little sensitivity to the annual cycle because the annual subduction rates are the same in each case; $\mathscr{H}_{\text{sub}}$ reaches a maximum of ~ 20 W m^{-2} in the center of the gyre. We now use our idealized subduction experiments to test and understand the contribution of the two potential sources of buoyancy $\mathscr{H}_{\text{net}}$ and $\mathscr{H}_{\text{pump}}$ to this subduction process.

1) How does the mixed-layer cycle affect the annual mean heating?

The thermodynamic balance of the mixed layer, written in terms of $\mathscr{H}_{\text{net}}$, is

$$h\left\{\frac{\partial \rho_m}{\partial t} + \mathbf{u}_s \cdot \nabla \rho_m\right\} = -\frac{\alpha_E}{C_w}\mathscr{H}_{\text{net}},$$

where $\mathbf{u}_s$ is the geostrophic velocity at the sea surface. The variables can be separated into annual-mean and seasonal components; thus,

$$h(t) = \bar{h} + h'(t),$$
$$\rho_m(t) = \overline{\rho_m} + \rho_m'(t),$$
$$\mathbf{u}_s(t) = \overline{\mathbf{u}_s} + \mathbf{u}_s'(t),$$
$$\mathscr{H}_{\text{net}}(t) = \overline{\mathscr{H}_{\text{net}}} + \mathscr{H}'_{\text{net}}(t).$$

Now assuming

- a local relation between the mixed layer depth and density, that is,

$$h(x, y, t) = h(x, y, \rho_m),$$

and

- the surface velocity varies little over the seasonal cycle, that is,

$$|\mathbf{u}_s'| \ll |\overline{\mathbf{u}_s}|;$$

it follows that the mean thermodynamic balance is

$$\bar{h}(\overline{\mathbf{u}_s} \cdot \nabla \overline{\rho_m}) + \overline{h'(\overline{\mathbf{u}_s} \cdot \nabla \rho_m')} \approx -\frac{\alpha_E}{C_w}\overline{\mathscr{H}_{\text{net}}}. \quad (20)$$

Downloaded from http://journals.ametsoc.org/doi/pdf/10.1175/1520-0485(1995)025<0138:OTTOS>2.0.CO;2 by guest on 06 August 2020

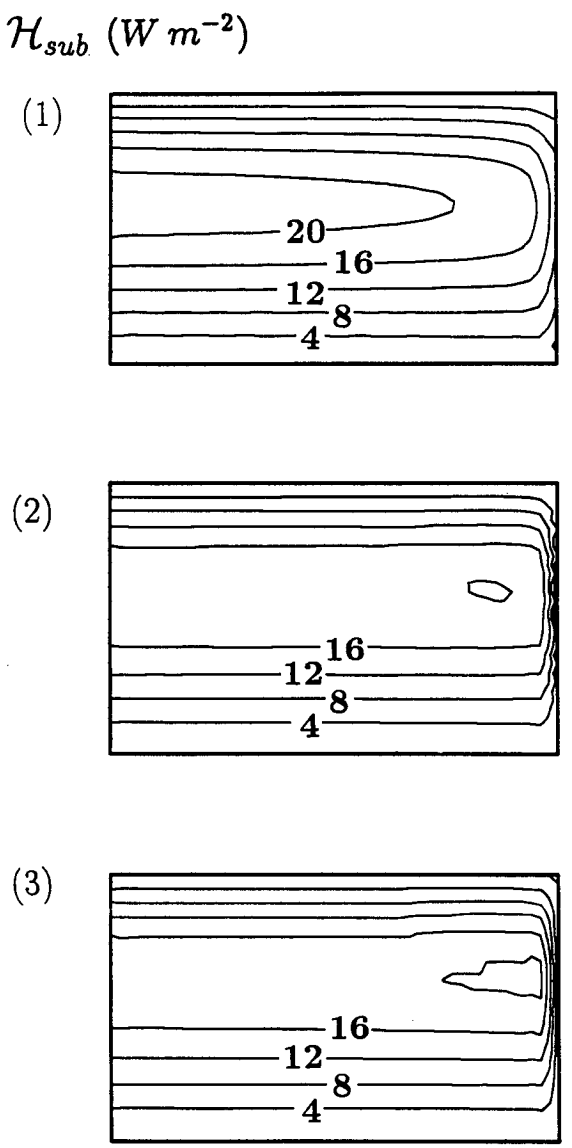

FIG. 11. The heat flux required by the annual subduction mechanism, $\mathscr{H}_{sub}$ (W m^{-2}).

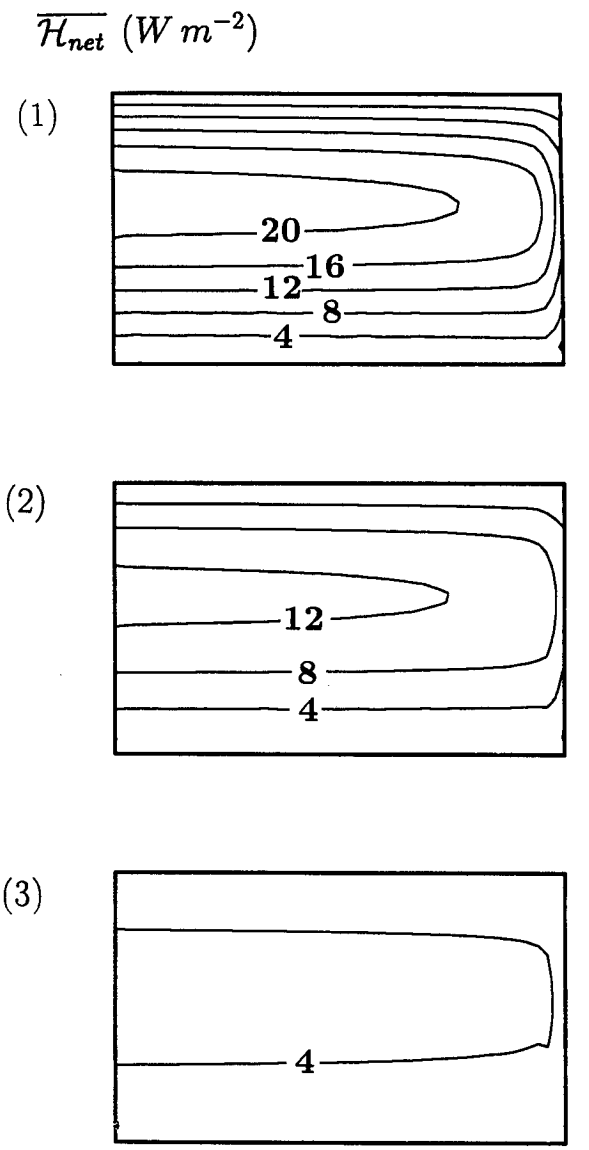

FIG. 12. Annual-mean net heating fields, $\overline{\mathscr{H}_{net}}$ (W m^{-2}). The annual-mean net heating is large in the steady limit (experiment 1) but much smaller with a realistic seasonal cycle (experiment 3).

In our model, and we expect in the ocean also, the dominant balance is between the first and third terms: *thus, the amount of heat required to warm the annual-mean mixed layer is proportional to the volume of fluid it contains:* as $\bar{h} \to 0$, $\overline{\mathscr{H}_{net}} \to 0$. The second term in (20) describes a correction arising because surface temperature gradients tend to be greater in summer when the mixed layer is shallow than in winter when the mixed layer is deep.

We plot $\overline{\mathscr{H}_{net}}$ in Fig. 12 for the three experiments: in experiment 1 where the mixed layer has winter properties and so is deep, $\overline{\mathscr{H}_{net}}$ is large ($\sim$20 W m^{-2}); in experiment 3 where the annual-mean mixed layer is shallow, $\overline{\mathscr{H}_{net}}$ is reduced to only 4 W m^{-2}. We thus see that we are able to obtain identical annual subduction rates in the three experiments, yet with strikingly different (and, for our most realistic seasonal cycle, near vanishing) $\overline{\mathscr{H}_{net}}$.

2) How important is $\mathscr{H}_{pump}$?

We have calculated $\mathscr{H}_{pump}$ in each of the experiments, and the results are shown in Fig. 13: they should be compared to $\mathscr{H}_{sub}$, Fig. 11, and $\overline{\mathscr{H}_{net}}$, Fig. 12. We find that $\mathscr{H}_{pump}$ is zero in experiment 1 and largest in experiment 3, as would be expected from Eq. (8b). The sum $\overline{\mathscr{H}_{net}} - \mathscr{H}_{pump}$ is fairly independent of the seasonal

Downloaded from http://journals.ametsoc.org/doi/pdf/10.1175/1520-0485(1995)025<0138:OTTOS>2.0.CO;2 by guest on 06 August 2020

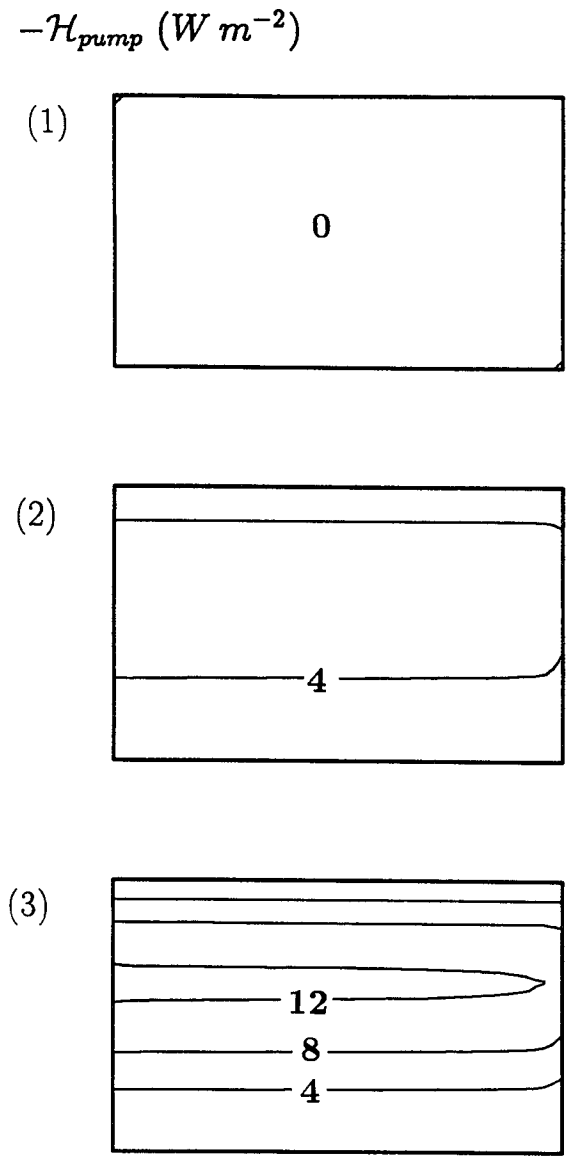

FIG. 13. The term, $-\mathscr{H}_{pump}$ (W m^{-2}), due to the downward pumping of fluid from the warm summer Ekman layer into the cooler seasonal thermocline. The sum $\mathscr{H}_{net} - \mathscr{H}_{pump}$ is similar in each experiment and in agreement with $\mathscr{H}_{sub}$ (Fig. 11).

cycle and is in general agreement with $\mathscr{H}_{sub}$; any discrepancy is a measure of the neglected terms arising from advection by the thermal wind within our fluid column. In experiment 1, the heating that supports annual subduction comes from the annual-mean net heat flux. However, in the most realistic limit—experiment 3—annual-mean net heating is small: the heat required to restratify the fluid column is pumped down from the warm summer Ekman layer into the cooler seasonal thermocline. This confirmation of the ideas of Federiuk and Price (1985) and MNW demonstrates the important role played by lateral Ekman heat fluxes in the annual subduction mechanism.

5. Discussion

We have discussed the thermodynamics attendant on the annual transfer of fluid between the surface mixed layer and the ocean thermocline. For a parcel of fluid in a weakly stratified mixed layer to enter into the main thermocline, it must be restratified by warming; this heat can be provided by either a flux through the sea surface and/or advective heat fluxes.

We have developed an idealized thermocline model in which a seasonally varying mixed layer is coupled with a continuously stratified thermocline in order to study the thermodynamic aspects of subduction. We find that in the most realistic limit characterized by a short season of deep winter mixing, the annual-mean net heat flux, defined in (3), is small: as suggested by climatological data (MNW), the buoyancy input that facilitates subduction is balanced by $\mathscr{H}_{pump}$, a pumping down of warm water from the summer Ekman layer into the cooler seasonal thermocline.

Our results have important implications for the interpretation of the surface heat flux, either imposed or diagnosed, in steady-state ocean models. In a subtropical gyre with no interannual variability, the total flux of heat into the gyre integrated over a year must identically vanish, irrespective of the seasonal cycle. However, as sketched in Fig. 2, this gyre-integrated flux consists not only of a radiative flux through the sea surface but also a lateral advection of heat through the boundaries separating the gyre from neighboring waters. In particular, the temperature of fluid fluxed into the subtropical gyre by surface Ekman processes varies significantly over the year: in a steady model with winter mixed layer conditions, *cold* fluid is fluxed into the gyre year-round, whereas in reality *warm* fluid is fluxed into the gyre during summer months. This *deficit* in the Ekman heat transports in a steady-state model must be compensated by an *enhancement* in the buoyancy flux into the ocean through the sea surface.

This result receives support from the recent inverse calculation of Marotzke and Wunsch (1994), in which an attempt is made to find a steady-state circulation of the North Atlantic consistent with observations. The surface heat flux required over the subtropical gyre is indeed found to be in excess of the observed mean heat flux. Whereas Marotzke and Wunsch ascribe this discrepancy to large uncertainties in the thermodynamic fluxes, we believe that this result is to be expected on physical grounds.

In a steady ocean model, it is necessary to parameterize the effects of the seasonal cycle on the Ekman heat transports. One approach is to evaluate $\mathscr{H}_{pump}$ directly from observations and to force the model with an effective heat flux, $\mathscr{H}_{sub} = \overline{\mathscr{H}_{net}} - \mathscr{H}_{pump}$. Alternatively one might prescribe the temperature and depth of the mixed layer from observations, as in the idealized models of Williams (1989, 1991) and Huang (1990);

Downloaded from http://journals.ametsoc.org/doi/pdf/10.1175/1520-0485(1995)025<0138:OTTOS>2.0.CO;2 by guest on 06 August 2020

the diagnosed net heat flux must then be interpreted as the combined contribution of $\overline{\mathscr{H}_{\text{net}}} - \mathscr{H}_{\text{pump}}$.

Acknowledgments. We should like to thank Ric Williams for many helpful discussions. We are also grateful to the reviewers whose comments led to a substantially improved manuscript. Financial support was provided by NSF 9115915-OCE.

APPENDIX

Method of Solution

a. Characteristic equation for ρ_m

Suppose, at time t, that the mixed layer density field is known through integration of (17). One can invert the potential vorticity field $Q(\rho)$ to find the depth of any isopycnal surface $z(\rho)$ relative to the bowl, $z = -D(x, y, t)$, on which density takes up its reference value, $\rho = \rho_D(D)$ (e.g., see Nurser 1988). Thus, integrating (12) in the vertical,

$$z(\rho) = -D + f\int_{\rho}^{\rho_D} \frac{d\rho}{Q(\rho)}. \tag{A1}$$

As yet the bowl depth remains unknown. However, Sverdrup balance, Eq. (14), after integrating by parts, transforming the vertical coordinate, and using the eastern boundary condition, Eq. (15), can be rewritten [see Williams 1989, Eq. (30)] in the following form:

$$\frac{2\bar{\rho}f^2}{\beta g}\int_{x_e}^{x} w_{\text{Ek}}\,dx = \int_{\rho_m}^{\rho_D} (z^2 - z_0^2)\,d\rho. \tag{A2}$$

The only unknown in (A1) and (A2) is the bowl depth, $D(x, y, t)$; we solve the coupled equations, (A1) and (A2), for $D(x, y, t)$ using a root-finding algorithm due to Brent (1973).

Having determined the bowl depth, the depth of each isopycnal surface can be determined directly from Eq. (A1), and in particular, setting $\rho = \rho_m$ provides the depth of the mixed layer

$$h = D - f\int_{\rho_m}^{\rho_D} \frac{d\rho}{Q(\rho)}. \tag{A3}$$

The surface pressure can also be written [see Eq. (10) of MN] in terms of integrals of z,

$$p_s = -g\int_{\rho_m}^{\rho_D} (z - z_0)\,d\rho - g\int_{\rho_{m_0}}^{\rho_m} z_0\,d\rho, \tag{A4}$$

and can be evaluated using Eq. (A1).

Thus, employing the above procedure, we can deduce each term in the thermodynamic equation, (9), from a prior knowledge of only the mixed layer density. This enables one to reduce Eq. (9) to a single characteristic equation in ρ_m:

$$\frac{\partial \rho_m}{\partial t} + \mathbf{u}_{\mathbf{c}} \cdot \nabla \rho_m = \mathscr{F}, \tag{A5}$$

where

$$\mathbf{u}_{\mathbf{c}} = \frac{1}{\rho_0 f}\,\mathbf{k} \times \nabla p_s + \frac{1}{h}\,\mathbf{U}_{\text{Ek}}$$

and

$$\mathscr{F} = -\frac{\alpha_E \mathscr{H}_{\text{in}}}{C_w h}.$$

Using prescribed patterns of wind and buoyancy forcing, Eq. (A5) can be integrated along characteristics to solve for $\rho_m(t)$.

b. Solutions with a prescribed $h(t)$

In section 4 we present solutions in which the mixed layer depth cycle $h(t)$ is prescribed, and the net heat flux is diagnosed. The method of solution has to be modified slightly.

Equations (A1), (A2), and (A3) now form coupled equations for ρ_m and D, which we can again solve using the root-finding algorithm of Brent (1973). Having deduced the mixed layer density field we can evaluate the surface pressure from (A4). Finally, rearranging Eq. (A5) gives

$$\mathscr{H}_{\text{net}}(t) = -\frac{hC_w}{\alpha_E}\left\{\frac{\partial \rho_m}{\partial t} + \frac{1}{\rho_0 f}\,\mathbf{k} \times \nabla p_s \cdot \nabla \rho_m\right\}, \tag{A6}$$

from which we can diagnose the net heat flux as a function of time.

REFERENCES

Bleck, R., H. P. Hanson, D. Hu, and E. B. Kraus, 1989: Mixed layer–thermocline interaction in a three-dimensional isopycnic coordinate model. *J. Phys. Oceanogr.*, **19,** 1417–1439.

Brent, R. P., 1973: *Algorithms for Minimization without Derivatives,* chapters 3 and 4, Prentice-Hall.

Cushman-Roisin, B., 1987: Subduction. *Dynamics of the Oceanic Surface Mixed Layer,* P. Muller and D. Henderson, Eds., Hawaii Institute of Geophysics Special Publications, 181–196.

Dewar, W., 1989: A theory of the time-dependent thermocline. *J. Mar. Res.*, **47,** 1–31.

Federiuk, J. M., and J. F. Price, 1985: Mechanisms of oceanic subduction. Unpublished manuscript.

Huang, R. X., 1990: On the three-dimensional structure of the wind-driven circulation in the North Atlantic. *Dyn. Atmos. Ocean.*, **15,** 117–159.

Liu, Z., and J. Pedlosky, 1994: Thermocline forced by annual and decadal surface temperature variation. *J. Phys. Oceanogr.*, **24,** 587–608.

Luyten, J. R., J. Pedlosky, and H. Stommel, 1983: The ventilated thermocline. *J. Phys. Oceanogr.*, **13,** 292–309.

Marotzke, J., and C. Wunsch, 1994: Finding the steady state of a general circulation model through data assimilation: Application to the North Atlantic Ocean. *J. Phys. Oceanogr.*, in press.

Marshall, D., 1992: Dynamics of the North Atlantic subtropical gyre. Ph.D. thesis, Imperial College, University of London, 206 pp.

Marshall, J. C., and A. J. G. Nurser, 1991: A continuously stratified thermocline model incorporating a mixed layer of variable thickness and density. *J. Phys. Oceanogr.*, **21,** 1780–1792.

Downloaded from http://journals.ametsoc.org/doi/pdf/10.1175/1520-0485(1995)025<0138:OTTOS>2.0.CO;2 by guest on 06 August 2020

——, and ——, 1992: Fluid dynamics of oceanic thermocline ventilation. *J. Phys. Oceanogr.*, **22,** 583–595.
——, ——, and R. G. Williams, 1993: Inferring the subduction rate and period over the North Atlantic. *J. Phys. Oceanogr.*, **23,** 1315–1329.
Nurser, A. J. G., 1988: The distortion of a baroclinic Fofonoff gyre by wind forcing. *J. Phys. Oceanogr.*, **18,** 243–257.
——, and J. C. Marshall, 1991: On the relationship between subduction rates and diabatic forcing of the mixed layer. *J. Phys. Oceanogr.*, **21,** 1793–1802.
Rhines, P. B., and W. R. Young, 1982: A theory of wind-driven circulation. I. Mid ocean gyres. *J. Mar. Res.*, **40**(Suppl.), 559–596.
Stommel, H., 1979: Determination of watermass properties of water pumped down from the Ekman layer to the geostrophic flow below. *Proc. Natl. Acad. Sci. U.S.*, **76,** 3051–3055.
Williams, R. G., 1989: The influence of air–sea interaction on the ventilated thermocline. *J. Phys. Oceanogr.*, **19,** 1255–1267.
——, 1991: The role of the mixed layer in setting the potential vorticity of the ventilated thermocline. *J. Phys. Oceanogr.*, **21,** 1803–1814.
——, M. A. Spall, and J. C. Marshall, 1995: Does Stommel's demon work? *J. Phys. Oceanogr.*, submitted.
Woods, J. D., 1985: The physics of thermocline ventilation. *Coupled Atmosphere–Ocean Models,* J. C. J. Nihoul, Ed., Elsevier, 543–590.

journals.ametsoc.org/doi/pdf/10.1175/1520-0485(1995)025<0138:OTTOS>2.0.CO;2 by g